

Electronic Supplementary Information

Dipeptides-bonded stationary phases for hydrophilic interaction liquid chromatography

Magdalena Skoczylas, Szymon Bocian, Bogusław Buszewski

Chair of Environmental Chemistry and Bioanalytics, Faculty of Chemistry, Nicolaus Copernicus University, Gagarin 7, 87-100 Torun, Poland, Fax: +48 56 611 4837; Tel: +48 56 611 4308, e-mail: bbusz@chem.umk.pl

Experimental

Instruments

The liquid chromatograph was a Shimadzu Prominence system (Tokyo, Japan) equipped with ternary gradient pump (LC-20AD), diode array detector (SPD-M20A), an autosampler (SIL-20A), and a column thermostat (CTO-10AS). Instrument control, data acquisition, and processing were performed with LabSolutions software for HPLC.

Elemental analysis was done using a Perkin-Elmer CHN 240 analyzer (Palo Alto, USA).

Thermogravimetric analysis (TGA) was performed on a Simultaneous TGA-DTA SDT 2960 thermal analyzer (TA Instruments, New Castle DE, United State). The bare silica (5.882 mg), silica modified with aminopropyl groups (Silica-Amino; 8.269 mg), Amino-Gly (8.923 mg), and Amino-Ala materials (12.180 mg) were heated from room temperature to 1000°C at a rate of 10°C/min in air atmosphere.¹

Solid state ¹³C NMR measurements, before and after chemical modification, were performed on a Bruker Avance III 700 MHz (Karlsruhe, Germany) after placing ca. 300 mg samples in the double-bearing rotors of zirconia. The ¹³C cross-polarization magic-angle spinning (CP MAS) NMR spectra were received with rotation frequency 8 kHz, pulse time 2 ms, acquisition time 0.01643 s, and relaxation time 6 s.

FTIR spectra in the range $\tilde{\nu} = 4000 - 400 \text{ cm}^{-1}$ were recorded on a Spectrum 2000 instrument (Perkin-Elmer Norwalk, USA). The data of this measurement was described elsewhere.²

The synthesized adsorbents were packed into 125 × 4.6 mm i.d. stainless steel tubes (Sigma Aldrich, Germany), using the slurry method. Around 1.5 g of the modified material was prepared as a suspension with 15 ml of methanol and put into the packing apparatus. Acetonitrile was used as a packing pressurizing solvent during the filling process. Both columns were packed using a DSF 122 packing pump (Haskel INC, USA) under a pressure of a 40 MPa.

Materials and method

The solid support of laboratory-prepared stationary phases was Kromasil 100, with particle diameter 5 μm, pore diameter 100 Å, pore volume 0.9 ml/g, surface area 310 m²/g (Kromasil, Eka Chemicals, AKZO NOBEL, Bohus, Sweden). Silica gel was chemically modified with aminopropyl groups with a coverage density $\alpha_{NH_2} = 3 \text{ } \mu\text{mol/m}^2$.³ The following reagents were used for chemical modification of the silica support: Fmoc-Gly-OH, Fmoc-Ala-OH, N,N'-dicyclohexylcarbodiimide (DCCI), piperidine, anhydrous dichloromethane (DCM), anhydrous N,N-dimethylformamide (DMF) (Sigma-Aldrich, St. Louis, MO, USA). The following organic solvents were used during synthesis: methanol, and toluene (J.T. Baker, Deventer, The Netherlands). In this study the commercially available Luna HILIC column, 150 × 4.6 mm with particle diameter 5 μm (Phenomenex, Torrance, California, U.S.) was also used for the comparison.

Binary mobile phase consisting of acetonitrile and water was applied in chromatographic analysis. Organic solvent was of high purity “for HPLC” (Sigma-Aldrich, St. Louis, MO, USA). Water was purified using a Milli-Q system (Millipore, El Paso, TX, USA) in our laboratory. Ammonium acetate (NH₄Ac) was obtained from Sigma-Aldrich (St. Louis, MO, USA).

All of the analyses were performed at 30°C, using acetonitrile as an organic modifier in the mobile phase, with the UV detection at 254 nm. The analytes were tested in HILIC conditions. As test samples, the mixture of nucleosides (8 purines and 4 pyrimidines) and the mixture of nucleic bases were used (AppliChem GmbH, Darmstadt, Germany).

Results and discussion

Elemental analysis

Synthesized stationary phases were characterized by elemental analysis. Table S1 shows results of chemical modification of the silica gel surface, i.e. content of carbon, nitrogen, and hydrogen, after each bonding reaction, determined by elemental analysis. The resulting data allows for the calculation of bonded ligand coverage density, based on the equation derived by Berendsen.⁴

The data presented in Table S1 confirms bonding of individual amino acids, due to the increase of carbon, nitrogen and hydrogen contents in the synthesized stationary phases. Final materials that were used for further investigation contain two bonded amino acids (Amino-Gly² and Amino-Ala² in Table S1). The percentage of nitrogen in the Amino-Ala phase is slightly larger than Amino-Gly phase, which demonstrates the bonding of more molecules of amino acids. The above relations are also reflected in the values of the surface coverage of amino acid groups, which equal 1.73 and 2.90 $\mu\text{mol}/\text{m}^2$ for Amino-Gly and Amino-Ala, respectively. Due to the steric hindrance, the coverage of bonded peptide ligands is lower than the primary coverage density of amino groups. Additionally, the lower (about 49%) carbon content after the first step of modification relative to the second stage suggests that the bonding of amino acids could occur via two active centers. One of them was an amino group embedded from already bonded amino acid, which resulted in the formation of a layer of dipeptide. The bonding of amino acids could also occur on the unbonded amino groups of the support. Therefore, the synthesized stationary phases are characterized by a heterogeneous surface of chemically bonded ligands.

NMR spectroscopy

The chemically bonded ligand structure was investigated by ¹³C CP/MAS NMR spectroscopy. Figure S2 presents the spectra obtained for the synthesized stationary phases. In the case of spectrum received for Amino-Gly material (Figure S2A), four signals were observed. The signals 6 and 7, which were distinguished by the largest value of chemical shifts ($\delta=174$ ppm), were ascribed to the carbon atoms on the carbonyl groups. Theoretical value of chemical shift for such group is in the range $\delta=150 - 180$ ppm.⁵ Furthermore, the small signal intensity is characteristic of the quaternary carbon, due to the absence of proton, which prevents intensification of ¹³C NMR signal.

The other signals were assigned to carbon atoms derived from an aliphatic system, for which the signals are recorded up to $\delta=60$ ppm. The chemical shifts are modified by the presence of different substituents. Thus, the presence of amino groups in the proximity of carbon atom (signal 4, $\delta=45$ ppm) changes the location of signals in the direction of lower values of the chemical shifts scale. The alteration of chemical shift is caused by the shielding effect associated with the presence of the electron-donor substituent (-NH₂). This type of moiety causes an increase in the electron density around the carbon atom. Therefore, the magnetic field acting on the carbon atoms is of greater intensity, and we observe a lower value of the chemical shift.

The signals 3 and 5 around $\delta=45$ ppm correspond to the carbon atom linked to the amide group. The nitrogen atom involved in the interaction with the oxygen of the carbonyl group has no effect of substituent I-type. Accordingly, the signals appear in the position defined by the position of the aliphatic carbon atoms. Further, the signal at $\delta=23$ ppm was assigned to the methylene group not linked to a heteroatom (signal 2). The carbon atom connected to silicon gives a signal indicated by peak at $\delta=11$ ppm.

The spectrum obtained for Amino-Ala phase (Figure S2B) is characterized by a greater number of signals compared to the ones previously discussed. In the low value of chemical shifts scale signals from alkyl groups are observed. However, due to the reduction of shielding effect, methylene groups not connected to a heteroatom have a higher value of chemical shift $\delta=24$ ppm (signal 2) than methyl groups with corresponding signals at $\delta=22$ ppm (signals 8 and 9). The smallest chemical shift of $\delta=11$ ppm is characterized by a carbon atom linked to a silicon atom (signal 1). Signals in the range of $\delta=47-50$ ppm were attributed to carbon atoms linked with nitrogen atoms (signals 3-5). Similarly as in the previous spectrum, the carbonyl carbon atoms have chemical shifts of $\delta=175$ ppm (signals 6 and 7). Furthermore, the signals R and R' are the spinning side bands of carbonyl carbon signal.⁵⁻⁹

FTIR spectroscopy

The structures of peptide-silica stationary phases were also confirmed using FTIR spectroscopy. Table S2 presents a detailed analysis of FTIR spectra obtained for amino-bonded silica, Amino-Gly, and Amino-Ala stationary phases. On each spectrum the weak signal which corresponds to amino groups derived from aminopropyl ligands may be found at around $\tilde{\nu}=1600$ cm^{-1} . Simultaneously, in that range a signal appears that corresponds to amide groups localized in a short alkyl chain. Additionally, bending and stretching vibrations of siloxane groups (-O-Si-O-) are responsible for the signals at $\tilde{\nu}=472-802$ cm^{-1} , and $\tilde{\nu}=1100$ cm^{-1} , respectively. The characteristic peak of peptide-silica packing spectrum at $\tilde{\nu}=1550$ cm^{-1} is assigned to the stretching vibrations of carbonyl group. In the spectrum of the Amino-Ala phase, an additional peak at $\tilde{\nu}=1454$ cm^{-1} corresponding to the methyl group is observed. The signals in the range of $\tilde{\nu}=3300-3700$ cm^{-1} are connected with residual silanols, amines, as well as water adsorbed on the surface of the stationary phase. It has to be also mentioned that these bands show the moisture content of the sample, which is characteristic of a compressed pellet method.^{1, 3, 10}

Thermogravimetric analysis (TGA)

The thermal stability of the silica and its modification, as well as immobilization of peptide ligands were measured by thermogravimetric analysis (TGA). The thermograms obtained for the materials of interest are shown in Figure S3. The TGA curve for native silica is characterized by two regions of weight loss. The initial process occurs in the 25°C – 132°C range (about 3.48% reduction of weight) and attributed to the thermodesorption of physically adsorbed water molecules from silica surface. The relatively equal weight in the temperature range from 132°C to 248°C, evident in the flat region of the TGA curve, is observed. The continuous heating led to the second weight loss region (from 248°C – 800°C) which was related to the dehydroxylation of the surface through the condensation reactions. This transformation of silica was associated with formation of siloxane bond, and loss of about 1.80% of chemically bound water.

The comparison of TGA curves for silica modifications and bare silica displayed significant differences. The initial weight loss from 25°C to 132°C decreased substantially, which is related to the smaller amount of physically adsorbed water on the surface of peptide materials. The main reason is the increasing hydrophobic properties of the packings, which leads to a decrease in the effective silanol concentration. Furthermore, in this range of temperature, the lowest (about 1.56%) reduction of mass for Amino-Ala with the highest coverage density of organic ligands was noted. These correlations also pertained to the reduction of volumes accessible for water, due to the bonding of large organic chains. The further weight loss occurs in the temperature range from 132°C to 376°C and corresponds to the condensation of silanol groups. The condensation process may be performed between neighboring aminopropyl moieties and peptide ligands, as well as residual surface silanols. The next transition in the temperature range

376°C – 650°C is justified since the thermal reduction of the mass came from the loss of organic moieties bonding to the silica. According to Figure S3, an increase of weight loss (including silanol condensation and thermal decomposition of ligands) in the order Silica-Amino, Amino-Gly, and Amino-Ala was presented. The highest reduction of weight ($\Delta TG_4 = 12.05\%$) for Amino-Ala material, due to the highest coverage density of peptide ligands, was noted. In contrast, the silica modified with the smallest organic moieties (Silica-Amino) lost only 4.59% (ΔTG_2) of weight. In the case of Amino-Gly material, the mass loss of 8.34% (ΔTG_3) was observed. It should be also noted that the TGA curves for silica modifications have various weight loss profiles, which shows the differences in the coverage density of peptide-materials. These correlations are also consistent with the results estimated through elemental analysis.^{1, 11-14}

1. S. Ray, M. Takafuji and H. Ihara, *J. Chromatogr. A*, 2012, **1266**, 43-52.
2. B. Buszewski, R. Gadzała-Kopciuch, R. Kaliszan, M. Markuszewski, M. T. Matyska and J. J. Pesek, *Chromatographia*, 1998, **48**, 615-622.
3. S. Bocian, A. Nowaczyk and B. Buszewski, *Anal. Bioanal. Chem.*, 2012, **404**, 731-740.
4. G. E. Berendsen and L. deGalan, *J. Chromatogr. A*, 1980, **196**, 21-37.
5. B. Buszewski, J. Schmid, K. Albert and E. Bayer, *J. Chromatogr. A*, 1991, **552**, 415-427.
6. B. Buszewski, R. M. Gadzała-Kopciuch, M. Markuszewski and R. Kaliszan, *Anal. Chem.*, 1997, **69**, 3277-3284.
7. K. Albert and E. Bayer, *J. Chromatogr. A*, 1991, **544**, 345-370.
8. B. Buszewski, Z. Suprynowicz, P. Staszczuk, K. Albert, B. Pfeiderer and E. Bayer, *J. Chromatogr. A*, 1990, **499**, 305-316.
9. R. M. Silverstein, F. X. Webster and D. J. Kiemle, *seventh ed.*, New York, 2005.
10. B. Buszewski, M. Jezierska, M. Wełniak and R. Kaliszan, *J. Chromatogr. A*, 1999, **845**, 433-445.
11. T. M. H. Costa, M. R. Gallas, E. V. Benvenuto and J. A. H. d. Jornada, *J. Non-Cryst. Solids*, 1997, **220**, 195-201.
12. Y.-L. Liu, W.-L. Wei, K.-Y. Hsu and W.-H. Ho, *Thermochim. Acta* 2004, **412**, 139-147.
13. R. Mueller, H. K. Kammler, K. Wegner and S. E. Pratsinis, *Langmuir*, 2003, **19**, 160-165.
14. C. P. Jaroniec, R. K. Gilpin and M. Jaroniec, *J. Phys. Chem., B* 1997, **101**, 6861-6866.

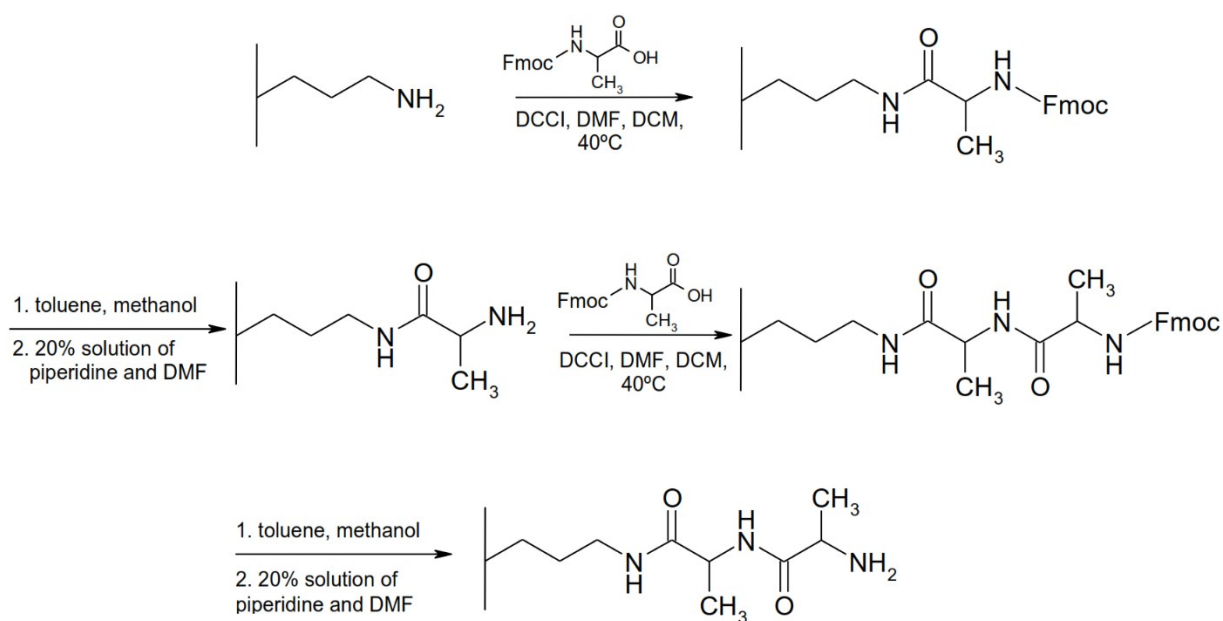


Figure S1 Synthesis of peptide-silica stationary phase comprising covalently bonded dipeptide of alanine.

Table S1 Physicochemical properties of peptide-silica stationary phases

Stationary phase*	Carbon content P _C [%]	Nitrogen content P _N [%]	Hydrogen content P _H [%]	Total coverage density of bonded amino acids [μmol/m ²]
Silica-Amino	3.013	0.920	1.059	3.00
Amino – Gly¹	3.971	1.372	1.057	1.73
Amino – Gly²	4.281	1.749	1.250	
Amino – Ala¹	4.036	1.391	1.098	2.90
Amino – Ala²	6.145	2.218	1.623	

¹ – product after first step of modification, ² – material after the second step of modification

Table S2 The analysis of FT IR spectra of received materials

Functional group	Type	Wavenumber ($\tilde{\nu}$) [cm ⁻¹]		
		SG-Amino	Amino-Gly	Amino-Ala
-O-Si-O-	bending	471	471	472
		804	802	802
-O-Si-O-	stretching	1104	1100	1104
-CH₃	bending	-	-	1454
-CH₂-	bending	-	-	1454
C=O	stretching	-	1550	1541
-NH₂	bending	1628	1666	1657
-NH-	bending	-		
C-H	bending	2944	2947	2943
-OH	stretching	3430	3381	3369

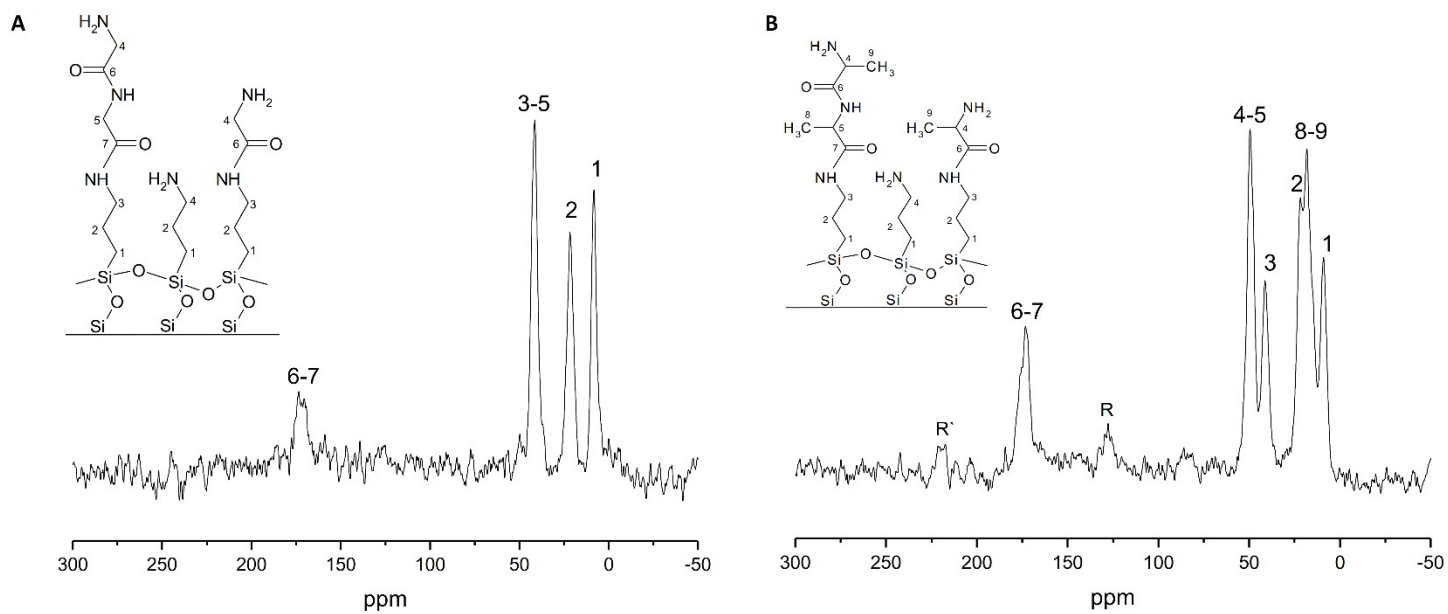


Figure S2 ^{13}C CP MAS NMR spectra of A – Amino-Gly and B – Amino-Ala.

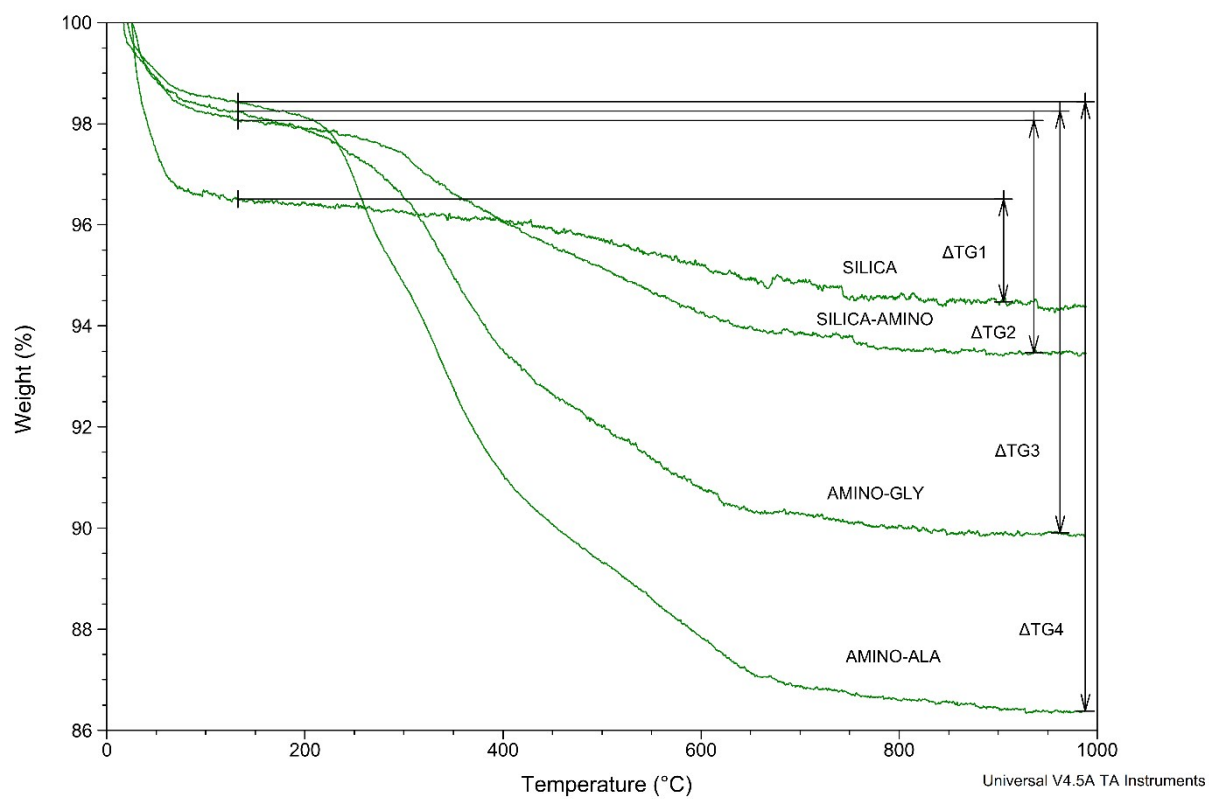


Figure S3 TGA thermograms of bare silica (Silica), silica modified with aminopropyl groups (Silica-Amino), Amino-Gly, and Amino-Ala materials in air atmosphere up to 1000°C.

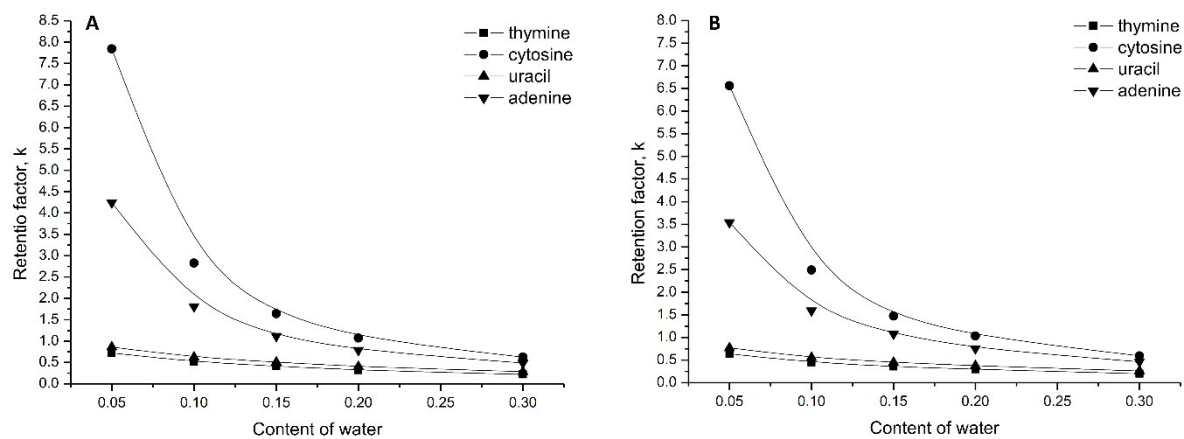


Figure S4 Effect of water content in the mobile phase on nucleic bases retention with utilization of Amino-Gly SP (A) and Amino-Ala SP (B). Conditions: mobile phase 20 mM NH_4Ac in $\text{ACN}/\text{H}_2\text{O}$, pH 6.51, flow rate, 1 ml min^{-1} , 30°C , $\lambda=254 \text{ nm}$.

Table S3 Chromatographic parameters of nucleosides separations. Conditions: mobile phase, ACN/H₂O (92/8), flow rate 1 ml min⁻¹, 30°C, λ=254 nm.

Compounds	Amino-Gly					Amino-Ala				
	k	N	R _s	A	f _{As} 10%	k	N	R _s	α	f _{As} 10%
2-deoxythymidine	1.19	4088	4.28	2.24	0.99	1.00	2784	2.82	2.01	0.75
1-methyladenosine	1.84	5148	4.42	1.55	1.00	1.37	3262	2.34	1.37	--
1-methylinosine	2.59	4338	3.98	1.41	0.94	1.62	1766	1.21	1.18	--
adenosine	3.21	1756	2.00	1.24	--	1.72	943	0.34	1.06	--
uridine	3.43	2576	0.60	1.07	--	1.91	3960	0.68	1.11	--
7-methylguanosine	4.25	6792	1.36	1.13	0.93	2.58	3075	3.06	1.36	0.71
1-methylguanosine	5.70	7539	2.99	1.23	0.94	3.27	295	1.10	1.27	--
pseudouridine	7.08	7656	4.07	1.24	--	3.50	1371	0.31	1.07	--
cytidine	7.80	7020	1.84	1.10	--	4.00	2825	1.16	1.14	--
8-bromoguanosine	8.30	7056	1.16	1.06	--	4.70	4936	2.01	1.18	--
N²-methylguanosine	12.16	8530	7.62	1.47	1.07	6.36	6012	4.69	1.35	0.85
guanosine	16.04	5888	5.31	1.32	1.13	10.04	4309	7.00	1.58	0.96